

# Synthesis, Characterization, and Viscoelastic Properties of High Molecular Weight Hyperbranched Polyglycerols

Rajesh Kumar Kainthan,<sup>†</sup> Edward B. Muliawan,<sup>§</sup> Savvas G. Hatzikiriakos,<sup>§</sup> and Donald E. Brooks<sup>\*,†,‡</sup>

Departments of Pathology & Laboratory Medicine, Chemistry, Chemical & Biological Engineering, and Centre for Blood Research, University of British Columbia, Vancouver, BC V6T 2B5, Canada

Received June 16, 2006; Revised Manuscript Received August 1, 2006

**ABSTRACT:** Very high molecular weight ( $M_n$  up to 700 000) and narrowly polydispersed (PDI = 1.1–1.4) hyperbranched polyglycerols (HPG) were synthesized by ring-opening multibranching polymerization of glycidol using dioxane as an emulsifying agent. Broader molecular weight distributions with low molecular weight fractions were obtained when diglyme was used as the emulsifying agent. But the low molecular weight fractions could be removed by dialysis. Isolated yields in both the cases were 70–90%. The different result in the case of dioxane may be due to faster cation exchange which leads to low polydispersities. HPGs of various molecular weights were characterized by a GPC system coupled with a multiangle laser light scattering detector and a triple detector array. The intrinsic viscosities were low for these polymers and did not increase with molecular weight. The dimensions of these polymers ( $R_g$ ,  $R_h$ ,  $R_\eta$ ) and their dependence on molecular weights are described. The hydrodynamic radii were very small with dimensions similar to those of dendrimers. Our results show that these polymers are very compact and have spherical conformations in water with no indications of aggregate formation. The melt viscoelastic properties were also studied. Despite their self-similar structures, depending on the type of solvent used to synthesize them (diglyme vs dioxane), topologically restricted configurations are produced that result in completely different entanglement dynamics.

## Introduction

Dendrimers show very interesting properties in the solid state and in solution because of their branching, globular shape, lack of entanglement, and large number of modifiable surface functional groups as well as internal cavities.<sup>1,2</sup> However, dendrimers are synthesized by tedious multistep reactions and purification steps and are therefore expensive, which is a major barrier to their bulk commercial applications. Hyperbranched polymers are built in a similar way to the dendrimers, but they have imperfectly branched structures.<sup>3–5</sup> The fact that hyperbranched polymers can be prepared in a convenient single step makes them potential alternatives to dendrimers in applications where a precise structure is not necessary, for example, in viscosity modification where the need is only for a globular structure or as cross-linking agents in coatings where the need is for a low-viscosity material with several reactive end groups. One of the major disadvantages of hyperbranched polymers is their large polydispersity.<sup>6</sup> However, recent theoretical work showed that controlled polymerization of  $AB_2$  monomers is possible by slow monomer addition.<sup>7,8</sup> Following this, controlled synthesis of hyperbranched polyglycerol (HPG) with low polydispersities and predetermined molecular weights was reported using anionic ring-opening multibranching polymerization of glycidol with slow monomer addition and partial deprotonation of the initiator.<sup>9</sup>

Because of their structural similarities with poly(ethylene glycol) (PEG) and polysaccharides, polyglycerols (PGs) are also expected to be biocompatible.<sup>10</sup> It is well-known that grafting or coating of PEG chains onto surfaces reduces platelet adhesion,

for instance, while coupling to drugs leads to longer plasma half-lives, reduced immunogenicity, and enhanced therapeutic efficacy.<sup>11–17</sup> The availability of functional groups in the PG class of polyether polyols suggests it as an attractive alternative to PEG in pharmaceutical and medical fields. Recently we reported the biocompatibility of these polymers using several *in vitro* techniques and animal toxicity studies where PGs were found to be as biocompatible as PEG.<sup>18</sup>

It has been theoretically predicted that for a polymer grafted surface, at equivalent areas per molecule, a branched polymer will be more efficient in reducing protein interactions with the coated surface than will be its linear analogue.<sup>19</sup> Recently, Haag and co-workers reported that hyperbranched polyglycerol self-assembled monolayers (SAMs) were as protein resistant as PEG SAMs.<sup>20</sup> An additional advantage is that HPG is thermally and oxidatively more stable than PEG.<sup>20</sup> This suggests that these robust polymers are promising as biomaterials.

One limitation of the studies with HPG reported to date has been their limitation to relatively low molecular weights ( $\sim 6000$  g/mol). Normally the synthetic reactions are done in the absence of solvent, but as the molecular weight of the polymer is increased above this range, the increment in viscosity becomes a barrier for efficient mixing, leading to broader polydispersity. The use of diethylene glycol dimethyl ether (diglyme) as an inert emulsifying solvent to reduce the viscosity of the polymerization mixture has been reported to provide HPGs with narrow polydispersity and close to theoretical molecular weights.<sup>21</sup> Molecular weights up to 20 000 g/mol have been reported by this method. As the number of functional groups approximately equals the degree of polymerization, synthesis of higher molecular weight HPGs is of significant interest as such materials would have numerous applications and would likely have properties unattainable by other approaches, given the difficulty in synthesizing higher generation dendrimers.

\* Corresponding author: e-mail don.brooks@ubc.ca; Fax (604) 822-7742.

<sup>†</sup> Department of Pathology & Laboratory Medicine and Centre for Blood Research.

<sup>‡</sup> Department of Chemistry.

<sup>§</sup> Department of Chemical and Biological Engineering.

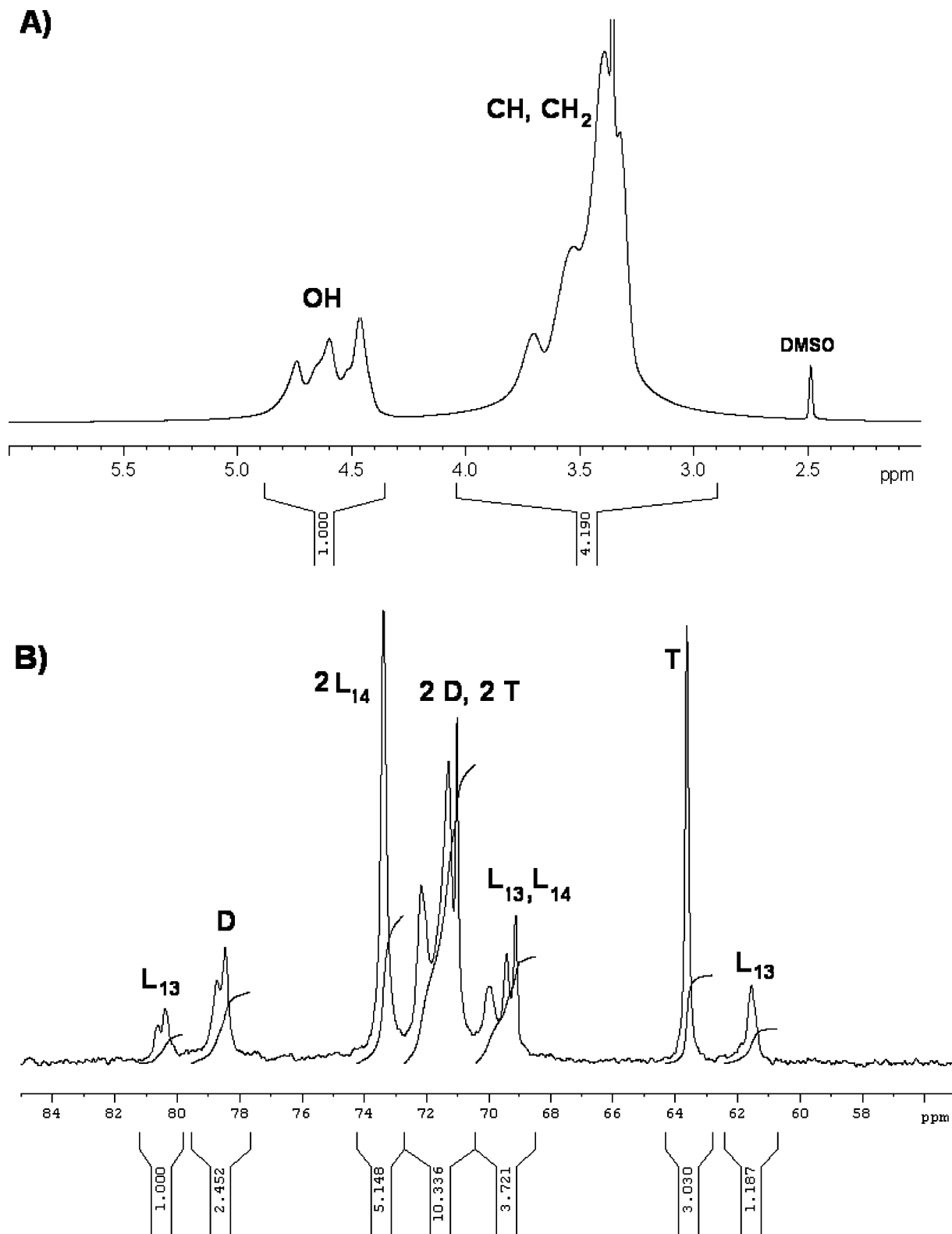


**Figure 1.** NMR spectra (DMSO-*d*<sub>6</sub>) of HPG-6 synthesized in diglyme: (A) <sup>1</sup>H spectrum; (B) <sup>13</sup>C inverse gated spectrum. Carbons corresponding to the terminal, dendritic, linear 1,3, and linear 1,4 units are denoted by T, D, L<sub>13</sub>, and L<sub>14</sub>, respectively.

In this report we describe the synthesis of very high molecular weight HPGs with low polydispersity using high monomer-to-initiator ratios in the presence and absence of emulsifying solvents. Such polymers, with low intrinsic viscosity and a very large number of derivatizable hydroxyl groups, may find applications in nanotechnology and in nanobiotechnology. The rheological properties of this series of novel hyperbranched

polyglycerols are also reported and analyzed. The polydispersity index of most of these polymers is relatively low ( $PDI = M_w/M_n = 1.1-1.8$ ), where  $M_w$  and  $M_n$  are the weight and number molecular weights, respectively, and the  $M_w$  range from 4000 to 1 475 000. The structures realized statistically approach the so-called Cayley tree molecular architecture (see Scheme 1) similar to branched polystyrenes studied by Dorgan et al.<sup>22</sup>

In the present case the molecular unit between branches is constant and therefore allows for a close examination of the effect of branching on the rheological properties.

## Experimental Section

**Materials and Methods.** All chemicals were purchased from Sigma-Aldrich Canada Ltd. (Oakville, ON) and used without further purification except as follows. Glycidol (96%) was purified by vacuum distillation and stored over molecular sieves in a refrigerator (2–4 °C). Anhydrous diglyme and dioxane were obtained from Aldrich and used without further drying. NMR spectra were recorded on a Bruker Avance 400 MHz NMR spectrometer using deuterated solvents (Cambridge Isotope Laboratories, 99.8% D) with the solvent peak as a reference. Molecular weights and polydispersities of polyglycerol samples were determined by gel permeation chromatography (GPC) on a Waters 2690 separation module fitted with a DAWN EOS multiangle laser light scattering (MALLS) detector from Wyatt Technology Corp. with 18 detectors placed at different angles (laser wavelength = 690 nm) and a refractive index detector (Optilab DSP from Wyatt Technology Corp.). An Ultrahydrogel linear column with bead size 6–13  $\mu\text{m}$  (elution range  $10^3$ – $5 \times 10^6$  Da) and an Ultrahydrogel 120 with bead size 6  $\mu\text{m}$  (elution range  $150$ – $5 \times 10^3$  Da) from Waters were used. An aqueous 0.1 N  $\text{NaNO}_3$  solution was used as the mobile phase at a flow rate of 0.8 mL/min. The  $dn/dc$  value for polyglycerol was determined to be 0.12 in aqueous 0.1 N  $\text{NaNO}_3$  solutions and was used for molecular weight calculations. The data were processed using Astra software provided by Wyatt Technology Corp.

Intrinsic viscosity  $[\eta]$ , viscometric radius ( $R_\eta$ ), Mark–Houwink parameters ( $a$  and  $K$ ), and radius of gyration ( $R_g$ ) were obtained from a triple detector from Viscotek Corp. connected to the GPC system, which utilizes refractive index, 90° light scattering, and intrinsic viscosity determinations. The data were processed using the software provided by Viscotek. Hydrodynamic radii ( $R_h$ ) were obtained from a quasi-elastic light scattering (QELS) detector (Wyatt Technology Corp.), which is connected to the MALLS detector, and these data were analyzed using the Astra software.

The triple detector viscometer consists of four capillary Wheatstone bridge configurations. The specific viscosity  $\eta_{sp}$  is calculated from the equation

$$\eta_{sp} = \frac{4\Delta p}{p_i - 2\Delta p} \quad (1)$$

where  $\Delta p$  is the differential pressure across the capillary bridge and  $p_i$  is the inlet pressure of the flow through the bridge. The intrinsic viscosity is calculated from

$$[\eta] = \eta_{sp}/c \quad (2)$$

as the concentration,  $c$ , is very low under GPC conditions. Initially, the viscometric radius of the molecule ( $R_\eta$ ) is calculated from

$$R_\eta = (3[\eta]M)^{1/3}(10\pi N_A)^{-1/3} \quad (3)$$

where  $M_w$  is the molecular weight calculated from the light scattering detector. The radius of gyration  $R_g$  is then estimated using the Flory–Fox and Ptitsyn–Eizner equations.<sup>23,24</sup>

$$R_g = \left(\frac{1}{6}\right)^{1/2} \left(\frac{[\eta]M_w}{\Theta}\right)^{1/3} \quad (4)$$

where  $\Theta = 2.55 \times 10^{21} (1 - 2.63\epsilon + 2.86\epsilon^2)$  and  $\epsilon = 2a - 1/3$  where  $a$  is the exponent of the Mark–Houwink equation

$$[\eta] = KM_w^a \quad (5)$$

The conformation coefficient  $\alpha$  is calculated from the relation

$$R_g = \beta M_w^\alpha \quad (6)$$

where  $\beta$  is a constant.

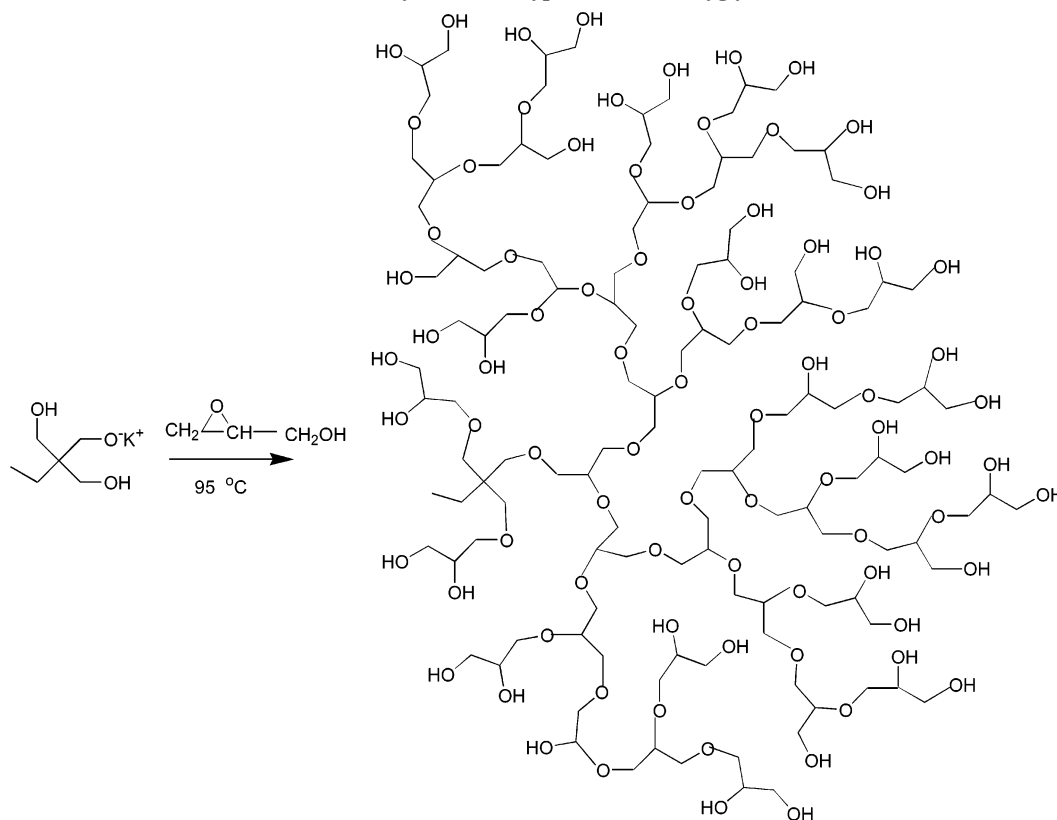
The linear viscoelastic experiments on HPG samples were performed using a stress-controlled (Bohlin C-VOR) rheometer equipped with 25 mm parallel plates. The characterization was done by performing frequency sweep experiments in the frequency range of 0.1 rad/s to about 500 rad/s. Dynamic stress sweep experiments were also performed to determine the regime of linear viscoelasticity. The tests were done at temperatures in the range of 25–100 °C. Time–temperature superposition was applied as necessary in order to obtain the master curves at the desired reference temperature, in this case  $T_{ref} = 100$  °C.

**Synthesis of High Molecular Weight Hyperbranched Polyglycerols.** Polymerizations were carried out in a three-neck round-bottom flask equipped with a mechanical stirrer. The second neck was connected to a dual manifold Schlenk line. The third one was closed with a rubber septum through which reagents were added. The polymerization procedure for a typical reaction was as follows. Initially trimethylolpropane (TMP) (0.187 g (1.39 mmol)); 1.68 g (12.5 mmol) in the case of HPG-1) was added to the flask under argon atmosphere followed by 0.11 mL of potassium methylate solution in methanol (20 wt %). Lower amounts of initiator were employed for higher molecular weights. The mixture was stirred using a magnetic stirrer bar for 15 min, after which excess methanol was removed in a vacuum until the bubbling stopped. Anhydrous diglyme or dioxane (20 mL) was added. The flask was kept in an oil bath at 95 °C, and 25 mL of glycidol (0.372 mol) was added dropwise over a period of 12 h using a syringe pump. After completion of monomer addition the mixture was stirred for an additional 5 h. It is to be noted that the initiator and the polymer are insoluble in either of the solvents which simply act as emulsifying agents to improve mixing. The product was dissolved in methanol, neutralized by passing three times through a column containing cation-exchange resin (Amberlite IRC-150). The polymer was then precipitated into excess of acetone and stirred for 2 h. Acetone was decanted out, and this procedure was repeated one more time. Dialysis of polymers was done for 3 days against water, changed three times a day, using cellulose acetate dialysis tubing (MWCO 1000 or 10 000 g/mol). The dry polymer was then obtained by freeze-drying.

## Results and Discussion

**Structure and Synthesis.** Hyperbranched polymers are generally globular in shape, and this compact shape leads to an absence of entanglements, unlike the case for linear polymers, which accounts for their low toughness. These amorphous materials therefore also possess low viscosity in bulk and in solution. Very high molecular weight HPGs with narrow polydispersity have not been reported yet. Because of the low viscosity and the high functionality, these polymers could find applications as cross-linkers, additives, or rheology modifiers. They could also find use as components in adhesives, advanced coatings, hydrogels, and composites. Other applications can be envisaged in catalysis, drug delivery, and nanotechnology. High molecular weight HPGs were synthesized in the presence and absence of an emulsifying agent. The  $^1\text{H}$  and  $^{13}\text{C}$  (inverse gated) NMR spectra are shown in Figure 1. A detailed characterization of low molecular weight polyglycerols by NMR has been described earlier.<sup>9</sup> The  $^1\text{H}$  and  $^{13}\text{C}$  NMR spectra of high molecular weight polyglycerols were similar to those reported for low molecular weight analogues. No significant difference in degree of branching was observed for HPG-6 and HPG-9, polymers made in two different solvents. The degree of polymerization cannot be determined from these spectra for the high molecular weight species as the difference between the integrals of terminal and dendritic units is too low to be accurate.

Scheme 1. Synthesis of Hyperbranched Polyglycerol

Table 1. Characteristics and Solution Properties of High Molecular Weight Hyperbranched Polyglycerols<sup>a</sup>

expt no.	solvent	theor $M_n$ $\times 10^{-3}$	yield (%)	$M_n \times 10^{-3}$	$M_w \times 10^{-3}$	$M_w/M_n$	$[\eta]^b$ (mL/g)	$R_h$ (QELS) (nm)	$R_g$ (TDA) (nm)	$R_h$ (TDA) (nm)	$\alpha$ (TDA)
HPG-1	none	3	86	3.4	4.1	1.2	3.2	nd	1.6	1.2	0.43
HPG-2	none	20	71	25	40	1.6	3.9	3.0	3.5	2.7	0.35
HPG-3	none	40	63	42.5	76.5	1.8	3.9	3.6	4.3	3.3	0.34
HPG-4	diglyme	20	81	106	217	2.0	3.6	3.9	6.2	4.8	0.27
HPG-5	diglyme	40	76	106	307	2.9	3.8	4.8	6.8	5.2	0.35
HPG-6	diglyme	40	68	266	771	2.9	3.8	6.6	9.3	7.2	0.37
HPG-7	diglyme	60	70	871	1475	1.7	3.8	7.8	12.5	9.6	0.39
HPG-8	dioxane	20	83	359	491	1.4	3.3	6.3	9.2	7.0	0.31
HPG-9	dioxane	40	90	540	589	1.1	3.0	6.8	9.2	7.1	0.34
HPG-10	dioxane	60	79	670	728	1.1	3.1	6.6	9.2	7.1	0.31

<sup>a</sup> Molecular weights from the MALLS data. <sup>b</sup> Intrinsic viscosity obtained from the viscotek data.

The polymers were characterized by a GPC/MALLS system and a triple detector system containing a refractive index detector, right angle light scattering detector, and a viscosity detector. The polymer characterization data are summarized in Table 1. The molecular weights and the polydispersity values were taken from the MALLS detector whereas the intrinsic viscosity values, viscometric radius, radius of gyration, and Mark-Houwink values were obtained from the triple detector system. The hydrodynamic radii were obtained from the QELS detector.

Initially we attempted to synthesize high molecular weight HPGs in bulk. Polymers of molecular weights 3000, 20 000, and 40 000 were targeted by employing higher monomer-to-initiator ratios, and fairly good control of molecular weights with polydispersities  $< 2$  was obtained. The chromatograms are shown in Figure 2. The polydispersity values were found to increase with molecular weight, perhaps due to the increase in viscosity of the reaction mixture as the stirring was difficult in the case of HPG-3. However, when diglyme was used as an emulsifying agent, high molecular weight polymers were obtained, but the polymers were found to have broader poly-

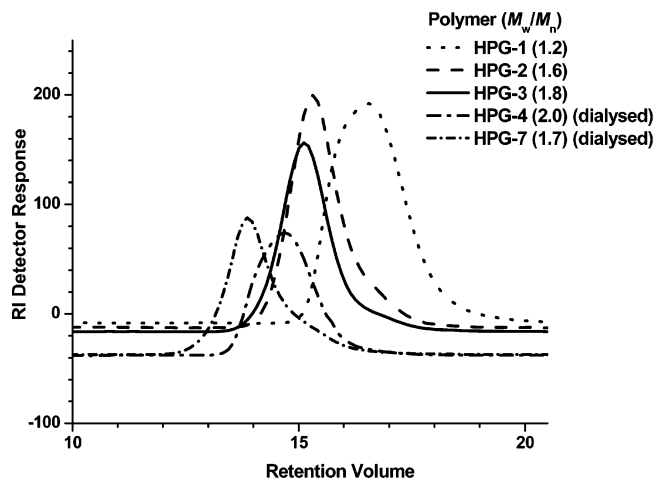
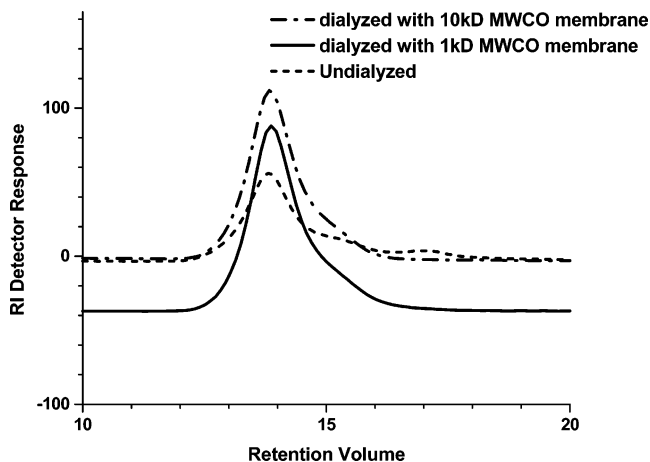
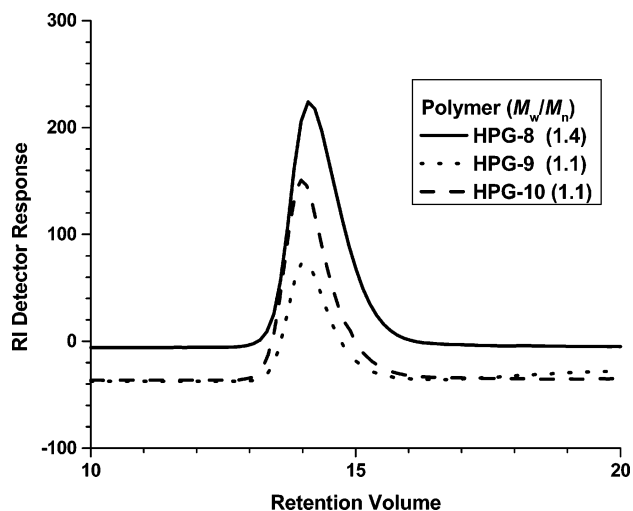


Figure 2. Chromatograms for the HPGs prepared in bulk and using diglyme as emulsifying agent.

dispersity with a low molecular weight tail in the GPC chromatogram. The low molecular weight fraction could be



**Figure 3.** Chromatograms for the high molecular weight HPG-7 before and after dialysis.



**Figure 4.** Chromatograms for the HPGs prepared using dioxane as emulsifying agent.

removed by dialysis, e.g., the polydispersity of HPG-4 reduced from 5 to 2.0 after 3 days of dialysis using a membrane of 1000 cutoff. Very high molecular weight polymers could be obtained by further increasing the ratio of monomer to initiator. The HPG-7 had a polydispersity of 4; the chromatogram is shown in Figure 3. Two low molecular weight fractions can be seen in the chromatogram. When this preparation was dialyzed using a 1000 MWCO membrane for 3 days, the lowest molecular weight fraction was removed, resulting in a polydispersity of 1.7 (Figure 3). The formation of higher molecular weights than the targeted values may be due to the small amounts of initiator and the presence of small amounts of moisture in the solvent. However, this shows that very high molecular weight polyglycerols with reasonably low polydispersities can be obtained using diglyme as an emulsifying agent.

We then tried dioxane as an emulsifying agent; the initiator and polymer are insoluble in this solvent. Surprisingly, we obtained very narrowly dispersed high molecular weight polymers with no need for dialysis. The GPC chromatograms are shown in Figure 4. The polymers were obtained by precipitation of a methanolic solution in acetone. The polydispersities were below 1.5 with monomodal distributions. The polydispersities of HPG-9 and HPG-10 were very narrow with  $PDI = 1.1$ . The sample HPG-9 was dialyzed (MWCO 1000), but this process did not change the molecular characteristics. Again the higher than expected molecular weights might be caused by a loss of

initiator due to the presence of moisture in the solvent. Our results show that very high molecular weight HPGs with low polydispersities can be obtained using dioxane as the reaction medium.

Limited deprotonation of TMP (only 10% of the total OH groups are deprotonated) and slow monomer addition are key to successfully controlling molecular weight with narrow polydispersity.<sup>9</sup> The polymerization proceeds with each alkoxide group reacting with the epoxide ring on its unsubstituted end, generating a secondary alkoxide and a primary alcohol group. Rapid cation exchange equilibrium between primary and secondary hydroxyl groups leads to chain propagation from all hydroxyl groups in the polymer chain, leading to a hyperbranched structure. An undesirable side reaction leads to macrocyclics which can be formed by the initiation of polymerization from a deprotonated glycidol monomer followed by propagation and intramolecular reaction of one of the alkoxide end groups with the epoxide group of the glycidol initiator. This is suppressed by slow monomer addition and by a faster propagation reaction. So, under identical polymerization conditions, the route to narrow polydispersity lies in the rapid cation exchange process. It is possible that since dioxane is a less polar solvent (dielectric constant,  $\epsilon = 2.2$ ) than diglyme ( $\epsilon = 7.0$ ), the exchange process is more favored, leading to more branched (discussed later) and narrowly dispersed polymers. In other words, with ions involved in the exchange process, such as, alkoxides,  $K^+$ ,  $H^+$  are more stabilized in a polar solvent such as diglyme compared to dioxane, decreasing the rate of cation exchange. This results in relatively broader polydispersity.

These high molecular weight HPGs are very interesting materials for applications utilizing further chemical manipulation owing to the presence of the very large number of hydroxyl groups. For example, HPG-10 which has a  $M_n$  of 670 000 has over 9000 OH groups. It is to be noted that this corresponds to a generation 11 PAMAM dendrimer. However, unlike the synthesis of a generation 11 dendrimer in 10 multisteps with same number of purification steps, these polymers were synthesized in a single step.

**Solution Properties.** We have prepared several polymers with different molecular weights, and their properties were studied as a function of molecular weight to establish a structure–property relationship. The low molecular weight polymers are viscous transparent liquids whereas the very high molecular weight analogues are opaque and hard, rubber-like materials. The polymers with molecular weight over 500 000 were insoluble in ethanol unlike those of lower molecular weight. However, all of them are easily soluble in polar solvents such as water, methanol, DMF, DMSO, and pyridine.

The solution properties of the polymers were studied by GPC analysis using the Viscotek triple detector, and the data were processed using TriSEC software (Viscotek). The analysis was done in aqueous 0.1 N  $NaNO_3$  solutions, and therefore the properties are not those of simple aqueous solutions. However, the properties of these polymers are not expected to depend significantly on the salt content. The intrinsic viscosity is a common parameter measured to describe the solution properties of a branched polymer, for instance to assess shrinkage due to branching. The average values of intrinsic viscosities and the weight-average molecular weights ( $M_w$ ) obtained from the MALLS data for each polymer are plotted in Figure 5. It can be seen from the graph that  $[\eta]$  does not change significantly with molecular weight. This is in agreement with earlier observations and is a characteristic feature of hyperbranched polymers.<sup>25,26</sup> The values varied from 3 to 4 mL/g. This

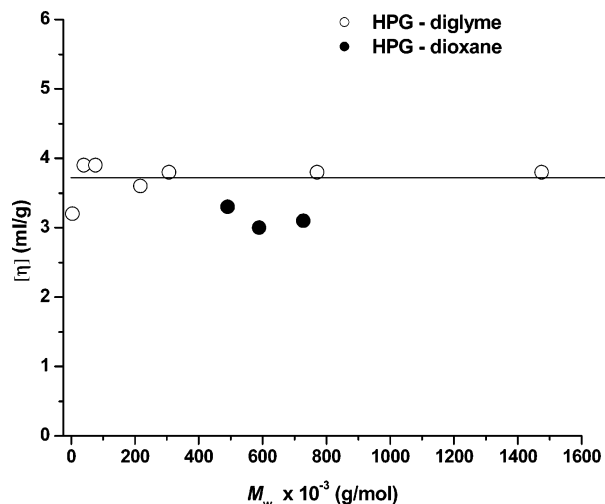


**Figure 5.** Intrinsic viscosity–weight-average molecular weight plot for HPGs.

constancy is consistent with a model in which the hyperbranched nature of the HPGs excludes flow from within the polymer, and the solution behaves according to the Einstein prediction for the intrinsic viscosity of suspensions of hard spheres.<sup>27</sup> This kind of behavior differs from that of dendrimers, which show a bell-shaped curve where  $[\eta]$  increases first as a function of molecular weight and then decreases after reaching a maximum.<sup>28,29</sup>

The linearity of the  $[\eta]$ – $M_w$  plot implies that the slope of the Mark–Houwink plot (the  $a$  parameter) is indistinguishable from zero. In general, the value of  $a$  decreases for polymers with compact structures and has a zero value for perfect hard spheres. For linear polymers with a random coil conformation,  $a$  has a value from 0.5 in a poor solvent to 0.8 in a good solvent. A value of 1 or greater is possible for extended rodlike structures. The HPG value of  $a = 0$  can be compared with the value of  $a$  for a poly(amido amine) (PAMAM) dendrimer, which is 0.237 in water.<sup>30</sup> It is to be noted that the polymers prepared in dioxane have lower intrinsic viscosities than those prepared in diglyme, suggesting they are more branched. Additional evidence for this structural difference is provided by the viscoelastic behavior and is discussed later. However, no significant differences in degree of branching were observed for any of these polymers by quantitative <sup>13</sup>C NMR spectroscopy, as mentioned earlier.

The hydrodynamic radii of the polymers were determined using a quasi-elastic light scattering (QELS) detector connected to the MALLS detector. The hydrodynamic radii increase from 2.5 to ~5 nm in the molecular weight range 20 000–200 000; above 200 000  $R_h$  increments only weakly, reaching 7–8 nm near a molecular weight of  $10^6$ . The small  $R_h$  values provide additional evidence for the absence of any intermolecular aggregation. The log–log plot of  $R_h$  vs molecular weight ( $M$ ) using the data obtained from the Astra software is shown in Figure 6A. The results of the linear regression using 1940 data points from all 10 polymers are also shown. The correlation coefficient  $r^2$  for the linear regression was 0.976 ( $p < 0.0001$ ). The scaling relation between  $R_h$  and  $M$  is  $R_h = 0.122M^{0.32}$ .

The values obtained for the hydrodynamic radii from QELS using dynamic light scattering agree well with the viscometric radii from the triple detector which uses intrinsic viscosity data (Figure 6B). Moreover, these values agree well with that reported for PAMAM dendrimers in methanol.<sup>31</sup> The scaling equation obtained using the  $R_h$  TDA data and the weight-average

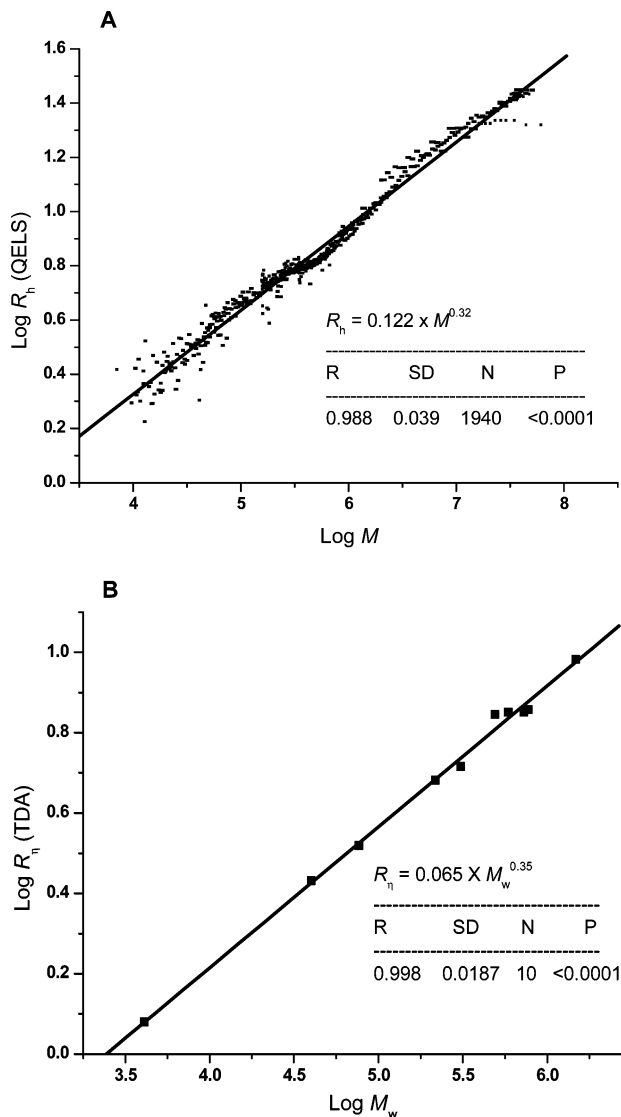


**Figure 6.** Log–log plot of the hydrodynamic radii vs weight-average molecular weight.

molecular weight of each polymer sample can be written as  $R_h = 0.065M_w^{0.35}$ . The values of the slope obtained from both the methods suggest that HPGs have spherical conformations; the values are similar to that reported for dendrimers.<sup>31</sup>

The radius of gyration is normally obtained from MALLS data. However, with the current instrumentation meaningful  $R_g$  values can only be obtained by MALLS if  $R_g \geq 10$  nm.<sup>32</sup> Therefore,  $R_g$  values were collected only for the high molecular weight chromatographic fractions whose values are above 10 nm. Double-logarithmic plots of  $R_g$  against  $M_w$  for HPG-7 and HPG-8 are shown in Figure 7. It can be seen that the plots are linear with indistinguishable slopes which suggests that these polymers, made in different solvents, possess self-similar structures. It is known that  $\alpha = 1.0$  for rigid rods, 0.58 for random coils in a good solvent, 0.5 for random coils in a  $\Theta$  solvent, and 0.33 for spheres.<sup>6</sup> The values of slopes  $\alpha$  (0.33–0.34), which are the conformation coefficients, again suggest that these polymers take on a spherical conformation. This value is in excellent agreement with the previously obtained value for HPGs (0.33) by neutron scattering.<sup>33</sup> While our observation is true for the higher molecular weights, it does not necessarily follow that the same result holds for lower molecular weights, however.<sup>6</sup>

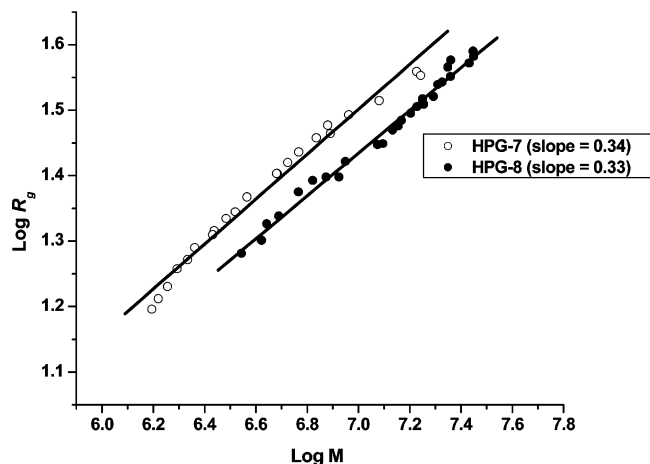


**Figure 7.** Plots of  $\log R_g$  vs  $\log M$  using MALLS data from the two polyglycerol samples.

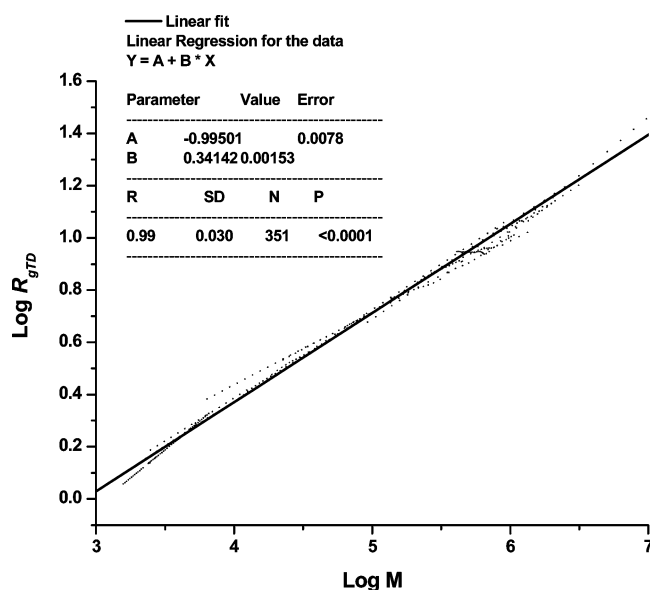


**Figure 8.** Plot of  $\log R_{gTD}$  vs  $\log M$  using data from all the polymers.

The triple detector is commonly used to obtain  $R_g$  values of polymers with values as low as 1 nm. The radii of gyration are calculated from the hydrodynamic radii using the appropriate model. We employed the random coil model to estimate the radius of gyration for ten polymers, designating the values  $R_{gTD}$  for values derived from triple detector data. This assumes that the behavior captured by eq 4 would provide the correct scaling for a hyperbranched material. This is only approximately correct, however, as it is known that the value of  $\Theta$  increases with the degree of branching due to a reduction in solvent draining.<sup>6</sup>

The relationship between  $R_{gTD}$  and molecular weight was established by plotting  $\log R_{gTD}$  vs  $\log M_w$  for the ten polymers (Table 1), and an overlay of plots is shown in Figure 8. All the plots fall on each other with no significant variation. The  $R_{gTD}$  values range from 1.0 to 16.0 nm, and the values are similar to that reported for dendrimers,<sup>31</sup> so the interpretation seems reasonable. The data from HPG-5 showed very high molecular weight fractions with  $R_{gTD}$  values up to 60 nm. Analysis of two broadly distributed high molecular weight polymers, HPG-5 and HPG-6, showed similar values. The results of the linear regression using 351 data points are also shown in Figure 8. The correlation coefficient for the linear regression was  $r^2 = 0.98$  ( $p < 0.0001$ ). The slope  $\alpha = 0.34$  again corresponds to a sphere and agrees well with the neutron scattering value reported

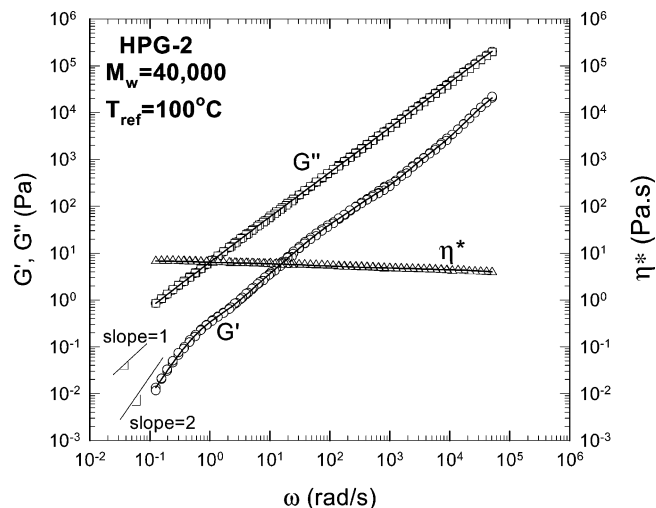


**Figure 9.** Dynamic spectra for sample HPG-2 referenced to  $T_{ref} = 100$  °C.

for HPGs of 0.33<sup>32</sup> and further supports the conclusion that these polymers are very compact in 0.1 N aqueous sodium nitrate solutions. The value for  $\alpha$  was relatively constant for over the whole range of molecular weights with a value of 0.43 for HPG-1, 0.35 for HPG-2, 0.34 for HPG-3, 0.27 for HPG-4, 0.35 for HPG-5, 0.37 for HPG-6, 0.39 for the HPG-7, 0.31 for HPG-8, 0.34 for HPG-9, and 0.31 for HPG-10.

The ratio of radius of gyration and hydrodynamic radius is commonly interpreted as an indicator of molecular compactness. The  $R_g/R_h$  ratios using values obtained for each high molecular weight fraction separated by GPC ( $R_g > 10.0$  nm) from MALLS and QELS data for HPG-7 and HPG-8 were calculated. The values ranged from 1.3 to 1.5, and averages of 1.42 (HPG-7) and 1.37 (HPG-8) were obtained. This observation again suggests that these polymers are all very similar with respect to their branching nature; i.e., intramolecular packing densities and molecular units between branches do not significantly differ. The value of  $R_g/R_h$  reported for a hard sphere is 0.78, 0.98 for a dendrimer ( $n > 10$ ), and 1.22 for a hyperbranched polymer chain, and for polydisperse populations of linear random coils in a good solvent the values are  $>2.0$ .<sup>6</sup> The values obtained here are closest to those for a related type of hyperbranched system, consistent with expectation.

**Viscoelastic Properties.** The linear viscoelastic properties of bulk HPG samples were studied using a stress-controlled rheometer. Figure 9 presents the master curves of the dynamic viscoelastic moduli of the HPG-2 sample as a representative of a low molecular weight HPG. The experiments were performed at several temperatures from 25 to 100 °C. The time-temperature superposition principle was successfully applied and produced master curves at the reference temperature of  $T_{ref} = 100$  °C. The dynamic storage modulus,  $G'$ , always remains below the loss modulus,  $G''$ . This implies that this sample is unentangled, mainly due to its low molecular weight ( $M_w = 40\,000$ ).  $G'$  and  $G''$  rise in parallel over 3 decades of frequency. The terminal zone at small frequencies has been reached with the characteristics slopes of 1 and 2 according to the scaling relationships  $G' \propto \omega^2$  and  $G'' \propto \omega$ , respectively. The dynamic viscosity,  $\eta^*$ , is independent of the frequency over this range of frequency (terminal zone). A small degree of shear thinning evidently appears at high shear rates.

Figure 10 presents the dynamic viscoelastic properties (moduli) of the HPG-4 sample as a representative of a medium

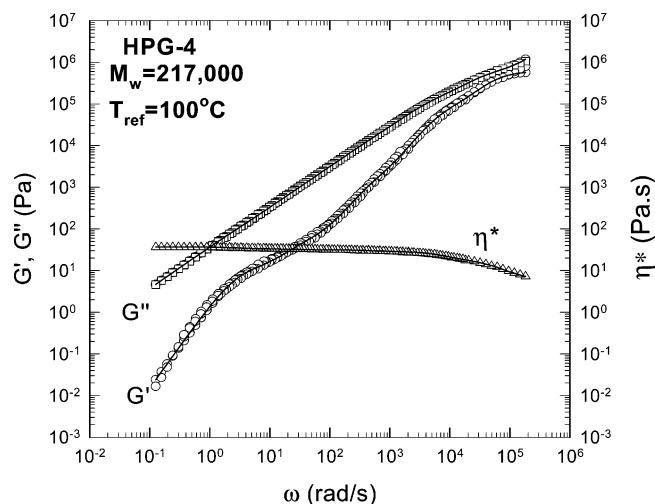


**Figure 10.** Dynamic spectra for sample HPG-4 referenced to  $T_{\text{ref}} = 100$  °C.

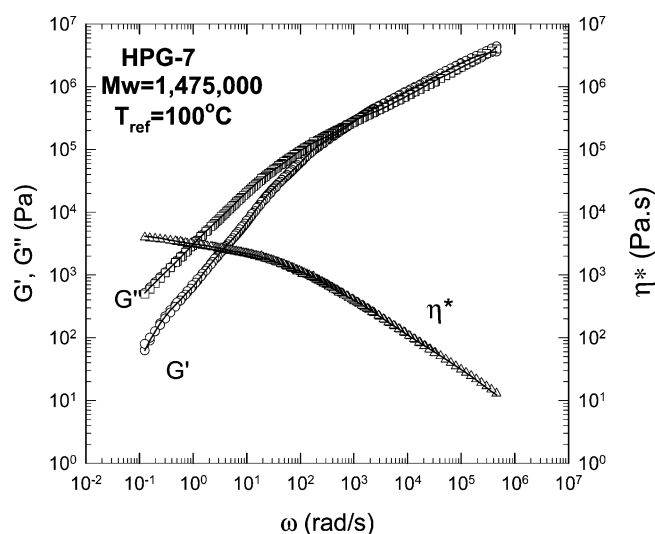


**Figure 11.** Dynamic spectra for sample HPG-7 referenced to  $T_{\text{ref}} = 100$  °C.

molecular weight ( $M_w = 217\,000$ ) at the reference temperature of  $T_{\text{ref}} = 100$  °C. Again, the dynamic storage modulus,  $G'$ , always remains below the loss modulus,  $G''$ , over the whole range of frequency. However, true entanglement dynamics are evident at high frequencies where the  $G'$  approaches  $G''$ . In fact, over a decade of frequency  $G'$  and  $G''$  increase in parallel with frequency with a characteristic slope of about 0.6. This behavior is referred to as “Zimm-like” with the slope predicted by the Zimm model to be  $2/3$ , which is very close to the experimental 0.6.

Evidence of high degree of entanglement and branching appears in the dynamic viscoelastic moduli of the HPG-7 sample (highest molecular weight) plotted in Figure 11. It can be seen that the  $G'$  and  $G''$  coincide at high frequencies and increase in parallel over more than 3 decades of frequency. This behavior is characteristic of gel-like and highly branched structures. The slope is 0.45, and similar exponents have been observed with other gels and hyperbranched systems.<sup>22,34–36</sup> The dynamic viscosity curves of both samples 4 and 7 clearly show shear thinning effects. The zero shear viscosity region has not been reached, and as described below it was obtained numerically.

Figure 12 plots the zero shear viscosity of all samples as a function of the molecular weight. These values were determined either experimentally (mainly for the low molecular weight

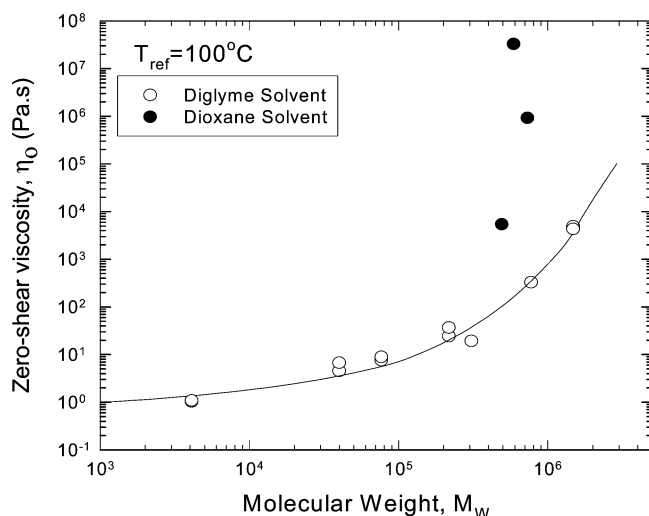


**Figure 12.** Scaling of the zero shear viscosity on the molecular weight of the polyglycerol polymers at  $T_{\text{ref}} = 100$  °C.

samples where the terminal zone was reached) or numerically (i) by making use of the discrete relaxation spectrum of the polymers (discussed in detail below) or (ii) by fitting a Carreau viscosity model to the viscosity data that includes the zero-shear viscosity as a fitting parameter. All these values (experimental and numerical) are plotted in Figure 12. An exponential expression seems to capture the scaling of the zero-shear viscosity with the molecular weight for the samples (open symbols) where diglyme was used as solvent. The equation describing the scaling of zero shear viscosity,  $\eta_0$ , with molecular weight,  $M_w$ , is  $\eta_0 = A \exp(BM_w^{0.5})$ , where  $A = 0.8$  Pa·s and  $B = 0.0069$  (mol/g)<sup>0.5</sup>, and appears in Figure 12 as a continuous line. Similar data on zero-shear viscosity showing exponential dependence on the molecular weight have been reported for star-branched polyisoprenes and other branched polymers.<sup>37</sup> More recently, a theoretical model to compute the rheological properties of branched polymers of varying architecture including polybutadiene combs, polyisoprene stars, and metallocene-catalyzed long branched polyethylenes was reported.<sup>38</sup> The zero shear viscosity predicted also implied an exponential dependence with the molecular weight.

It can also be seen from Figure 12 that the zero-shear viscosity of three samples produced with dioxane as an emulsifying agent cannot be described by the exponential equation. While all HPG polymers possess the same structure, possibly during polymerization, the presence of the hydrophobic dioxane produces molecular configurations that create highly branched configurations that are topologically “locked” or restricted in space. When these materials are solidified and then melted, they may retain some of the entanglements present in the solid, increasing the zero shear viscosity. While the degree of branching appears to be the same in all polymers, based on their self-similarity in solution,<sup>6</sup> the highly entangled polymers produced in dioxane appear to have a higher “effective” degree of branching retained in the melt. This effect is not seen when the polymers are dissolved, as there is no sign of aggregation in the SEC behavior for any of the preparations studied.

The dynamic moduli of HPG samples 9 and 10 are plotted in Figures 13 and 14, respectively. Their viscoelastic behavior is very different from that of HPG-7 although the molecular weight of HPG-7 (1 475 000) is much higher than those of HPG-9 and HPG-10 (589 000 and 728 000, respectively). It also evident that HPG-9 and HPG-10 are more entangled than HPG-7; the “locked” polymer configurations lead to an apparently

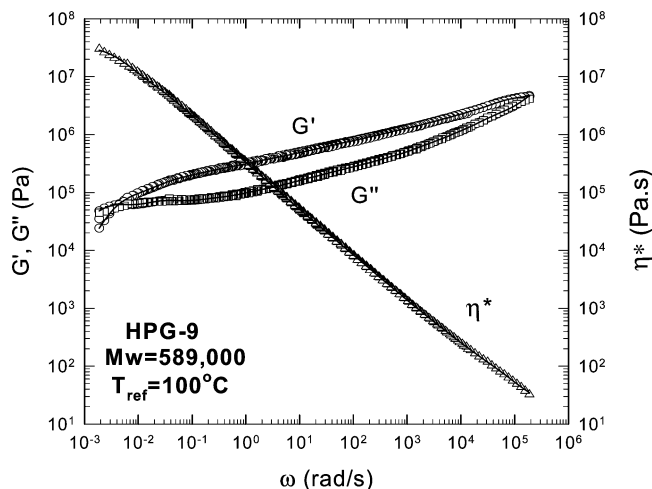


**Figure 13.** Dynamic spectra for sample HPG-9 referenced to  $T_{\text{ref}} = 100\text{ }^{\circ}\text{C}$ .

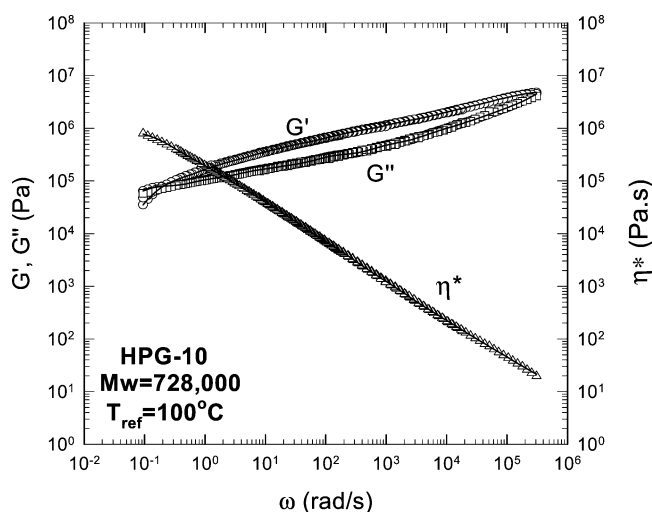


**Figure 14.** Dynamic spectra for sample HPG-10 referenced to  $T_{\text{ref}} = 100\text{ }^{\circ}\text{C}$ .

higher effective branching degree, as discussed above. This is also confirmed from Figure 5 where the intrinsic viscosities of samples HPG-8, -9, and -10 (filled symbols) are distinctly lower than those of the other samples, an indication of their higher “effective” degree of branching.

From Figure 13 the maximum which appears in the  $G''$  curve can be used to calculate the entanglement dynamics of these polymers. This value appears to be  $G''_{\text{max}} = 7.1 \times 10^4$  Pa. Using the well-established empirical relation  $G_N^0 = 4.83G''_{\text{max}}$  results in a plateau modulus of  $G_N^0 = 3.4 \times 10^5$  Pa. This result can be used to calculate the molecular weight between entanglements,  $M_e$ , and the critical molecular weight between entanglements,  $M_C$ . This can be done by using the Graessley–Fetters definition for the plateau modulus  $G_N^0 = (4/5)\rho RT/M_e$  which gives  $M_e = (4/5)\rho RT/G_N^0$  and the rule of thumb  $M_C \cong M_e$ . These equations provide  $M_e$  and  $M_C$  values of around 7500 and 15 000 for a density of  $1.28\text{ g/cm}^3$  at  $25\text{ }^{\circ}\text{C}$ . This agrees with the result of Figure 9 where HPG-3 with a molecular weight of 42 500 presents dynamics of an unentangled polymer melt. True entanglement dynamics start appearing at molecular weights greater than 200 000 (each molecule creates a few entanglements), i.e., in the case of HPG-4 plotted in Figure 10.

It should be mentioned that the shift factors used to superpose the data for all samples were about the same, showing the highly self-similar structure of all polymers. An Arrhenius type of

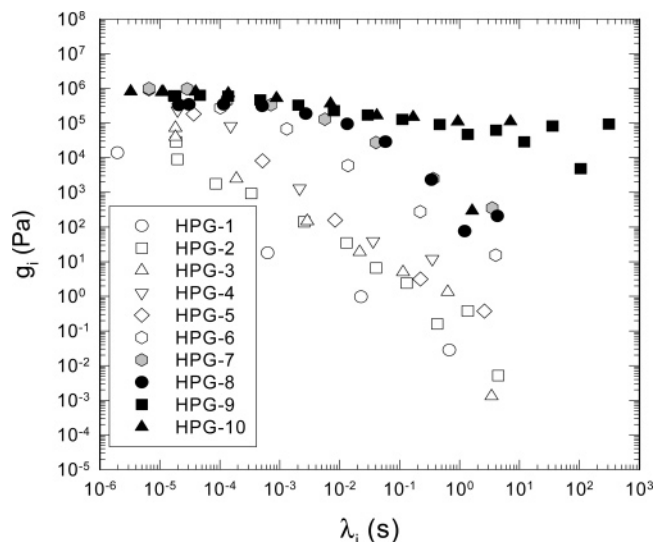


**Figure 15.** Discrete relaxation spectra of all HPG samples. Black symbols represent the spectra of the three HPG samples synthesized with use of the dioxane solvent ( $T_{\text{ref}} = 100\text{ }^{\circ}\text{C}$ ).

equation was used to describe these shift factors as

$$a_T = \exp\left(-\frac{E_a}{R}\left(\frac{1}{T} - \frac{1}{T_{\text{ref}}}\right)\right) \quad (7)$$

where  $E_a/R$  is the flow activation energy that characterized the sensitivity of the viscosity to temperature. Typical values of  $E_a/R$  ranging from 8018 to 9059  $\text{K}^{-1}$  were found with no particular trends observed among the various samples. For the high molecular weight polymers such as samples HPG-7, -9, and -10 vertical shift factors had to be used in order to obtain the excellent master curves. It is noted that vertical shift factors are typically used for branched polymers;<sup>39,40</sup> they mainly account for the effect of temperature on the polymer density.

The continuous lines which appear on Figures 9–11, 13, and 14 have been calculated using the discrete relaxation spectrum of each polymer. The linear viscoelastic moduli, the storage, and loss moduli can be described in terms of the discrete Maxwellian spectrum as<sup>41</sup>

$$G'(\omega) = \sum_i g_i \frac{(\omega\lambda_i)^2}{1 + (\omega\lambda_i)^2} \quad \text{and} \quad G''(\omega) = \sum_i g_i \frac{\omega\lambda_i}{1 + (\omega\lambda_i)^2} \quad (8)$$

where  $\omega$  is the frequency of oscillation and  $g_i$  and  $\lambda_i$  are the generalized Maxwell model parameters. The parameters ( $g_i$ ,  $\lambda_i$ ) of eq 8 are determined using a nonlinear optimization program following the algorithm developed by Baumgartel and Winter.<sup>42</sup> The program provides the least number of ( $g_i$ ,  $\lambda_i$ ) parameters (Parsimonious spectra) that best describe the results. These are plotted in Figure 15. Note the truncation of the spectrum to higher relaxation times with increase of the molecular weight. In particular for the three HPG samples produced in dioxane the spectrum is almost flat over 9 decades of time. In most cases, power-law expressions for the spectrum can be used.

## Conclusions

Very high molecular weight hyperbranched polyglycerols with narrow polydispersities were obtained by ring-opening multibranching polymerization of glycidol using dioxane as the reaction medium. No dialysis was needed. However, broader molecular weight distributions with low molecular weight

fractions were obtained when diglyme was used as the emulsifying agent. The polydispersity could be reduced by removing the low molecular weight fraction by dialysis against water. In both types of media the isolated yields were between 60 and 90%. The narrow polydispersity observed in the case of dioxane may be due to faster cation exchange compared to reaction in the more polar solvent diglyme. The properties of aqueous 0.1 N NaNO<sub>3</sub> solutions of all samples were consistent with expectations based on highly branched, nonaggregated structures, those produced in dioxane showing evidence from intrinsic viscosity data of being somewhat more compact (i.e., more highly branched) than those synthesized in diglyme. Owing to the presence of a large number of hydroxyl groups in a single polymer molecule (~12 000 OH groups in the case of HPG-5), these polymers may find many applications in nanotechnology and the biomedical area.

Linear viscoelasticity studies of the polymer melts revealed rich entanglement dynamics ranging from classical unentangled Rouse to highly entangled branched dynamics. Although all polymers possess a self-similar structure, use of the more hydrophobic (dioxane) vs a more hydrophilic emulsifying agent (diglyme) produced topologically restricted configurations that resulted in different viscoelastic behavior. The viscoelastic response of these materials was found to be similar to typical hyperbranched structures. Calculation of the plateau modulus resulted in an estimate of the critical molecular weight for the onset of entanglements of about 15 000 g/mol.

**Acknowledgment.** We thank the Canadian Institutes of Health Research, Natural Sciences and Engineering Research Council of Canada, the Canada Foundation for Innovation, B.C., Michael Smith Foundation for Health Research, Knowledge Development Fund, the Canadian Blood Services, and Bayer Canada Inc. for financial support.

## References and Notes

- (1) Oosterom, G. E.; Reek, J. N. H.; Kamer, P. C. J.; Van Leeuwen, P. W. N. M. *Angew. Chem., Int. Ed.* **2001**, *40*, 1828.
- (2) Frechet, J. M. J. *Macromol. Symp.* **2003**, *201*, 11.
- (3) Kim, Y. H.; Webster, O. J. *Macromol. Sci., Polym. Rev.* **2002**, *C42*, 55.
- (4) Sunder, A.; Heinemann, J.; Frey, H. *Chem.—Eur. J.* **2000**, *6*, 2499.
- (5) Gao, C.; Yan, D. *Prog. Polym. Sci.* **2004**, *29*, 183.
- (6) Burchard, W. *Adv. Polym. Sci.* **1999**, *143*, 125.
- (7) Hanselmann, R.; Hölter, D.; Frey, H. *Macromolecules* **1998**, *31*, 3790.
- (8) Radke, W.; Litvinenko, G.; Müller, A. H. E. *Macromolecules* **1998**, *31*, 239.
- (9) Sunder, A.; Hanselmann, H.; Frey, H.; Mulhaupt, R. *Macromolecules* **1999**, *32*, 4240.
- (10) Frey, H.; Haag, R. *Rev. Mol. Biotechnol.* **2002**, *90*, 257.
- (11) Zhang, F.; Kang, E. T.; Neoh, K. G.; Wang, P.; Tan, K. L. *Biomaterials* **2002**, *23*, 787.
- (12) Andrade, J. V.; Wei, A.-P.; Ho, C.-H.; Laea, A.; Jeon, S.; Lin, Y.; Straup, E. *J. Clin. Mater.* **1992**, *11*, 67.
- (13) Hoffman, A. S.; Stayton, P. S. *Macromol. Symp.* **2004**, *207*, 139.
- (14) Zalipsky, S. *Adv. Drug Delivery Rev.* **1995**, *16*, 157.
- (15) Mehvar, R. *J. Pharm. Pharm. Sci.* **2000**, *3*, 125.
- (16) Greenwald, R. B.; Choe, Y. H.; McGuire, J.; Conover, C. D. *Adv. Drug Delivery Rev.* **2003**, *55*, 217.
- (17) Duncan R.; Gac-Breton S.; Keane R.; Musila R.; Sat, Y. N.; Satchi, R.; Searle, F. *J. Controlled Release* **2001**, *74*, 135.
- (18) Kainthan, R. K.; Janzen, J.; Levin, E.; Dana, V.; Devine, D. V.; Brooks, D. E. *Biomacromolecules* **2006**, *7*, 703.
- (19) Irvine, D. J.; Mayes, A. M.; Griffith-Cima, L. *Macromolecules* **1996**, *29*, 6037.
- (20) Siegers, C.; Biesalski, M.; Haag, R. *Chem.—Eur. J.* **2004**, *10*, 2831.
- (21) Kautz, H.; Sunder, A.; Frey, H. *Macromol. Symp.* **2001**, *163*, 67.
- (22) Dorgan, J. R.; Knauss, D. M.; Al-Muallem, H. A.; Huand, T.; Vlassopoulos, D. *Macromolecules* **2003**, *36*, 380.
- (23) Fox, T. G.; Flory, P. J. *J. Am. Chem. Soc.* **1951**, *73*, 1904.
- (24) Ptitsyn, O. B.; Eizner, Y. E. *Sov. Phys. Technol. Phys.* **1960**, *4*, 1020.
- (25) Gauthier, M.; Li, W.; Tichagwa, L. *Polymer* **1997**, *38*, 6363.
- (26) Aharoni, S. M.; Crosby, C. R. I.; Walsh, E. K. *Macromolecules* **1982**, *15*, 1093.
- (27) Min, X.; Xiaohu, Y.; Cheng, R.; Yu, X. *Polym. Int.* **2001**, *50*, 1338.
- (28) Frechet, J. M. J. *Science* **1994**, *263*, 1710.
- (29) Mourey, T. H.; Turner, S. R.; Rubinstein, M.; Frechet, J. M. J.; Hawker, C. J.; Wooley, K. L. *Macromolecules* **1992**, *25*, 7261.
- (30) Tomalia, D. A.; Baker, H.; Dewald, J.; Hall, M.; Kallos, G.; Martin, S.; Roeck, J.; Ryder, J.; Smith, P. *Polym. J.* **1985**, *17*, 117.
- (31) Roovers, J.; Comanita, B. *Adv. Polym. Sci.* **1999**, *142*, 179.
- (32) Kim, S.; Cotts, P. M.; Volksen, W. *J. Polym. Sci., Part B: Polym. Phys.* **1992**, *30*, 177.
- (33) Garamus, V. M.; Maksimova, T. V.; Kautz, H.; Barriau, E.; Frey, H.; Schlotterbeck, U.; Mecking, S.; Richtering, W. *Macromolecules* **2004**, *37*, 8394.
- (34) Antonietti, M.; Pakula, T.; Bremser, W. *Macromolecules* **1995**, *28*, 4227.
- (35) Simon, P. F. W.; Muller, A. H. E.; Pakula, T. *Macromolecules* **2001**, *34*, 1677.
- (36) Roovers, J.; Graessley, W. W. *Macromolecules* **1981**, *14*, 766.
- (37) Graessley, W. W. *Acc. Chem. Res.* **1977**, *10*, 332.
- (38) Das, C.; Inkson, N. J.; Read, D. J.; Kelmanson, A.; McLeish, T. C. B. *J. Rheol.* **2006**, *50*, 207.
- (39) Shroff, R.; Mavridis, H. *J. Appl. Polym. Sci.* **1995**, *57*, 1605.
- (40) Hatzikiriakos, S. G. *Polym. Eng. Sci.* **2000**, *40*, 2279.
- (41) Dealy, J. M.; Wissbrun, K. F. *Melt Rheology and Its Role in Plastic Processing*; Van Nostrand Reinhold Co.: New York, 1990.
- (42) Baumgartel, M.; Winter, H. H. *Rheol. Acta* **1989**, *28*, 511.

MA0613483